The Use of Morphological Characteristics and Texture Analysis in the Identification of Tissue Composition in Prostatic Neoplasia

JAMES DIAMOND, PHD, NEIL H. ANDERSON, MD,
PETER H. BARTELS, PHD, FIAC, MD,
RODOLFO MONTIRONI, MD, FRCPATH, AND
PETER W. HAMILTON, PHD

Quantitative examination of prostate histology offers clues in the diagnostic classification of lesions and in the prediction of response to treatment and prognosis. To facilitate the collection of quantitative data, the development of machine vision systems is necessary. This study explored the use of imaging for identifying tissue abnormalities in prostate histology. Medium-power histological scenes were recorded from whole-mount radical prostatectomy sections at × 40 objective magnification and assessed by a pathologist as exhibiting stroma, normal tissue (nonneoplastic epithelial component), or prostatic carcinoma (PCa). A machine vision system was developed that divided the scenes into subregions of 100 × 100 pixels and subjected each to image-processing techniques. Analysis of morphological characteristics allowed the identification of normal tissue. Analysis of image texture demonstrated that Haralick feature 4 was the most suitable for discriminating stroma from PCa. Using these morphological and texture measurements, it was possible to define a classification scheme for each subregion. The machine vision system is designed to integrate these classification rules and generate digital maps of tissue composition from the classification of subregions; 79.3% of subregions were correctly classified. Established classification rates have demonstrated the validity of the methodology on small scenes; a logical extension was to apply the methodology to whole slide images via scanning technology. The machine vision system is capable of classifying these images. The machine vision system developed in this project facilitates the exploration of morphological and texture characteristics in quantifying tissue composition. It also illustrates the potential of quantitative methods to provide highly discriminatory information in the automated identification of prostatic lesions using computer vision. HUM PATHOL 35: 1121-1131. © 2004 Elsevier Inc. All rights reserved.

Key words: **histopathology, imaging, prostate, texture analysis.**

Abbreviations: **H_4, Haralick feature 4; PCa, prostatic carcinoma; PIN, prostatic intraepithelial neoplasia.**

Prostate cancer is set to become the most common cancer in men within the next 3 years.[1] New figures show that the incidence has been rising steadily since 1971, and if trends continue, it will overtake lung cancer before 2006. Around 22,000 cases of prostate cancer are diagnosed in the UK each year. New statistics show that deaths from prostate cancer have gradually declined since the early 1990s, but mortality is still high; 9500 men die from the disease each year in the UK.[1] A continuing challenge to the medical community is to develop successful strategies for treatment and early diagnosis of prostate cancer. It has been suggested that automated machine vision systems would form an element of this overall diagnostic strategy by providing improved accuracy and reproducibility of diagnosis.

This attractive concept has been around for many years now, but it has been limited to cytopathology, where progress has been made in developing cervical screening devices.[2,3] In histopathology, the development of automated systems has been lagging, essentially due to the complexity of imagery. Today, however, with developments in machine vision and intelligent image processing systems combined with advancements in computer hardware, the analysis of histopathologic images for the purpose of objective disease classification is now possible.[4-9]

The adoption of state-of-the-art quantitative methodologies by pathologists requires constant and active motivation. Baak[10] has suggested that the absence of this motivation by pathologists is a dominant factor hindering modernization of pathology. The objective of the present study was to investigate emerging methodologies in quantifying diagnostic pathology with the aim of increasing reproducibility and predictive accuracy in diagnosis. Baak[10] also suggested that these themes should not be "merely academically interesting," but should be required if the concept of objective diagnosis is to be embraced.

Central to this study is the generation of a representative image set conveying the varying tissue compositions observed in prostate histology. Images were preselected by a pathologist (N.A. and R.M.) as reflecting variation in stroma, normal tissue (nonneoplastic epithelial component), or prostatic carcinoma (PCa). The study assessed the use of quantitative methods in defining the criteria required for implementing an automated system capable of the unsupervised interpreta-

From the Biomedical Imaging and Informatics Research Group, The Queen's University of Belfast, Grosvenor Road, Belfast, Northern Ireland, UK; The Royal Hospital Trust, Belfast, Northern Ireland, UK; Optical Sciences Center, University of Arizona, Tucson, AZ; and Institute of Pathological Anatomy and Histopathology, University of Ancona, Ancona, Italy. Accepted for publication May 6, 2004.

Address correspondence and reprint requests to Dr. James Diamond, Biomedical Imaging and Informatics Group, The Queen's University of Belfast, Grosvenor Road, Belfast, BT12 6BL, Northern Ireland, UK.

0046-8177/$—see front matter

doi:10.1016/j.humpath.2004.05.010

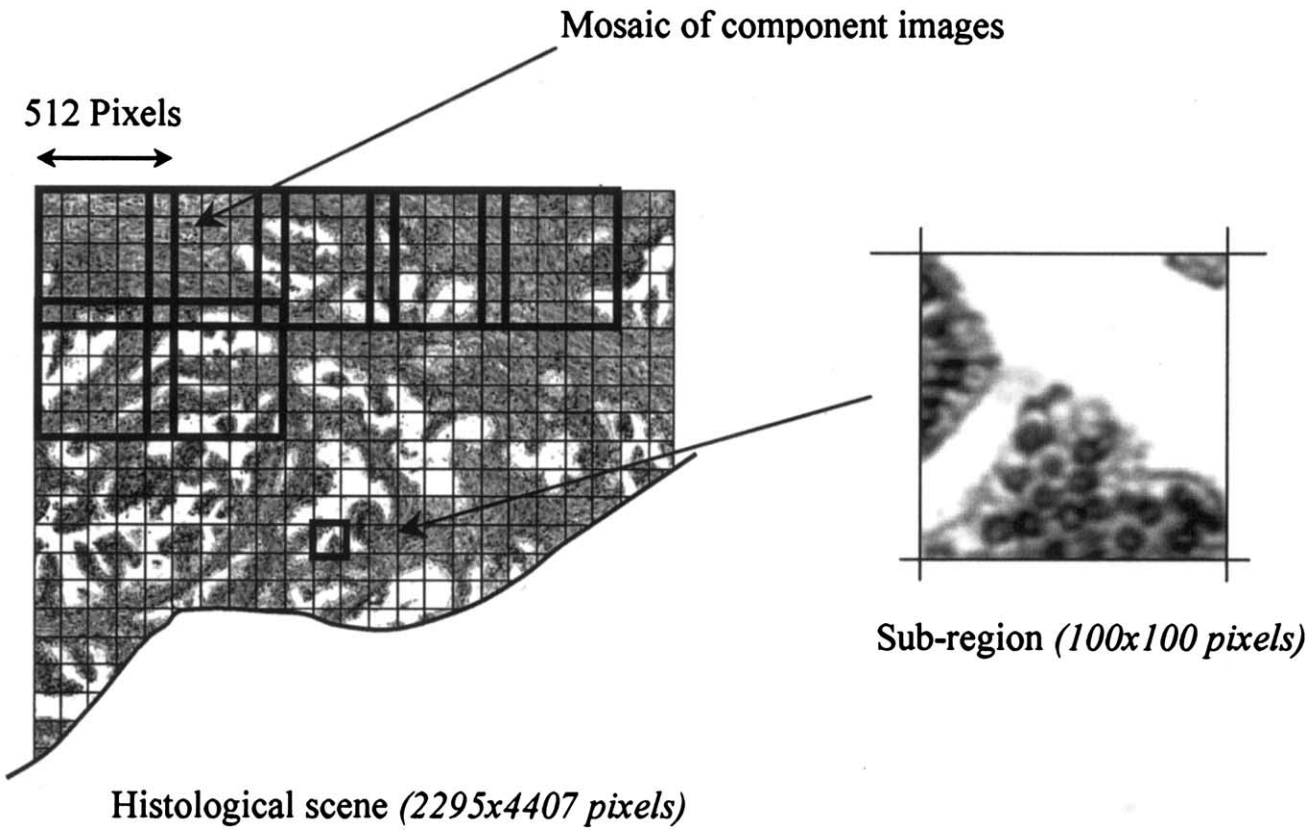

FIGURE 1. Histological scene description.

tion of histological scenes into the aforementioned groups on an objective basis.

Contextually, texture plays an important role in the perception of scenes and is used mainly to achieve image segmentation.[11] It has been used widely in the interpretation of prostatic ultrasound images[12,13] and in nuclear classification.[14-16] Previously it has been shown that texture analysis also provides an effective tool in tissue classification.[17-19] It has been suggested that texture analysis combined with image morphology can provide an effective tool for identifying tissue abnormalities in prostate histology.

MATERIALS AND METHODS

Tissue

Twelve cases (4 training and 8 test) from whole- mount radical prostatectomy sections that had been fixed in formalin embedded in paraffin, were retrieved from files at The Institute of Pathological Anatomy and Histopathology, University of Ancona, Italy. A set of 5-μm-thick sections were cut and stained with hematoxylin and eosin and assessed by pathologists (N.A. and R.M.) as showing regions of the following:

1. Stroma: Fibroelastic tissue containing randomly orientated smooth muscle bundles that act as a framework to support the prostatic architecture, morphologically forming a homogeneous texture within defined subregions
2. Normal tissue: Prostatic tissue with increased amounts of smooth muscle, glandular, and/or stromal components
3. PCa: Prostatic adenocarcinomas, histologically diverse and having more than one characteristic composition.

Implementation

Image analysis was implemented using the Zeiss KS400 imaging system (Carl Zeiss, Oberkochen, Germany). A methodology was designed to integrate image processing, texture analysis (after Haralick[20]), and classification rules for the generation of digital tissue composition maps.

Histological Scene Establishment

Twelve histological scenes were constructed by creating a seamless mosaic of component images (Fig 1). These images were captured at $\times$ 40 objective magnification using an Olympus BH2 microscope (Olympus, Lake Success, NY) and a Sony DX930P CCD camera (512 $\times$ 512 pixel, 8-bit, grayscale) (Sony, Ridge Park, NJ) and overlapped by 10% to allow for registration. The system was calibrated by adjusting the light source for an empty field until the mean field pixel value was 255 (white). Images often exhibit shading variation due to lighting irregularities, vignetting by the optical system, and heterogeneous sensitivity in the camera system or lens artifact. These effects were minimized by applying a shading

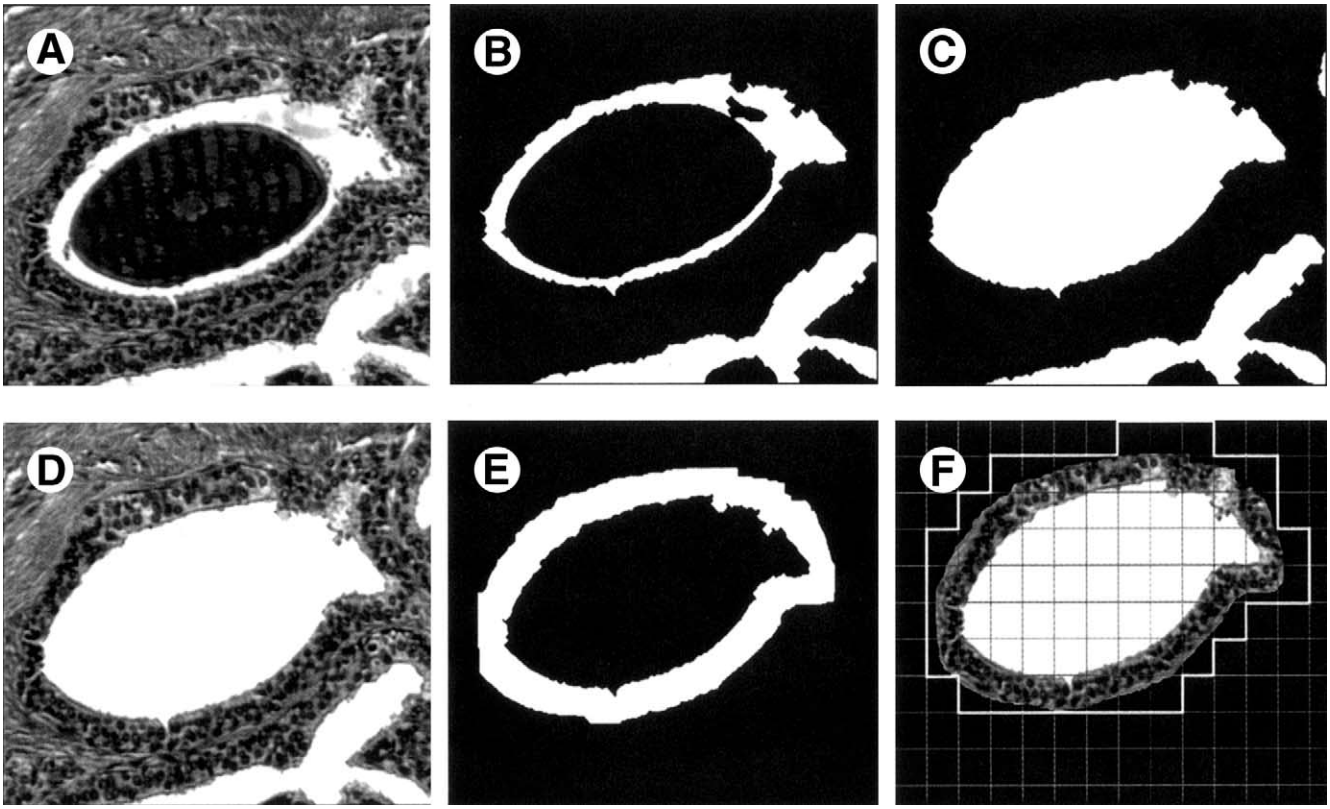

FIGURE 2. Gland processing and identification of regions exhibiting normal tissue. (A) Original gland. (B) Segmented lumen. (C) Debris removal. (D) Processed gland. (E) Epithelial layer. (F) Normal tissue assignment.

correction. Glandular preprocessing was implemented to remove intraluminal material (Fig 2). In subsequent tissue identification, the histological scenes were divided into subregions for processing. These subregions were sized to reflect the size and spatial relationships between and within pertinent objects (Fig 1).

Subregion Size Optimization

Processing the scene dictates that a subimage size be defined. Previous studies[17,21] have used a dimension of 256 × 256 pixels. However, texture analysis is based on the interrelationship between pixel intensities and is not related to the size of the subimage. For this reason, a subimage size was chosen to introduce a high degree of detail in defining the overall classification map; 100 × 100 pixels was chosen as optimal.

Classification Rules

Both texture and morphological characteristics of the scene were used in the classification of subimages. Texture is more appropriate for the identification of regions exhibiting greater homogeneity in structure. Consequently, in the present study, texture was used to distinguish between stroma and PCa. A morphological approach was applied to the classification of normal tissue, where the glandular tissue is heterogeneous in nature.

System Classification of Histological Scenes

In validating automated machine vision protocols, one must define a "gold standard" for classification. Consequently, 2 pathologists (N.A. and R.M.) independently assessed all histological scenes. From these assessments, continuous diagnostic maps were created reflecting the areas of stroma, normal tissue, and PCa. Subsequently, it was possible to define color-coded discrete maps based on the subregion size (100 × 100 pixels). The assigned color of the subregion in the discrete map was based on the predominant color in the corresponding subregion in the continuous map. To ensure that no glandular tissue was assigned as stroma, any subregion that had a glandular component of area >10% was assigned as normal tissue. Once the automated assessment of the histological scene was complete, a system discrete map was generated based on the classification of each subimage. Accuracy of the system was determined based on a subimage comparison between the pathologist and system discrete maps. Results from the classification were presented to the pathologist as numeric values and as a system continuous map created through image processing applied to the discrete map and superimposed on the scene (Fig 3).

RESULTS

Classification of Normal Tissue

The classification of normal tissue was achieved based on tissue morphological characteristics. The classification assumed that areas of normal tissue exhibit larger areas of associated lumen. Lumen were identified as in the preprocessing operation (Fig 2C). Interactive measurement of glandular structures (n = 50) from histological scenes (training set) established a

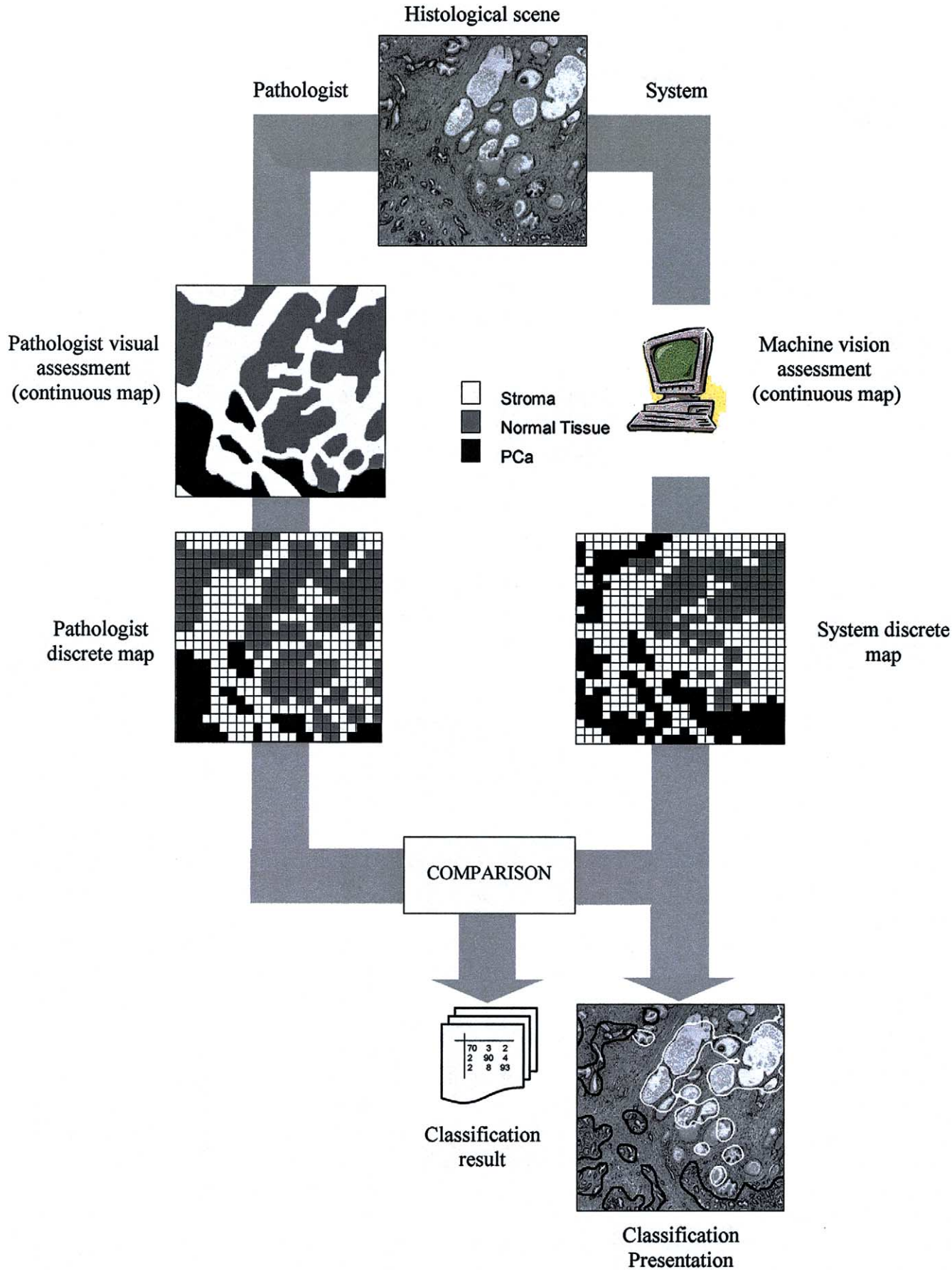

FIGURE 3. The identification and classification of tissue composition.

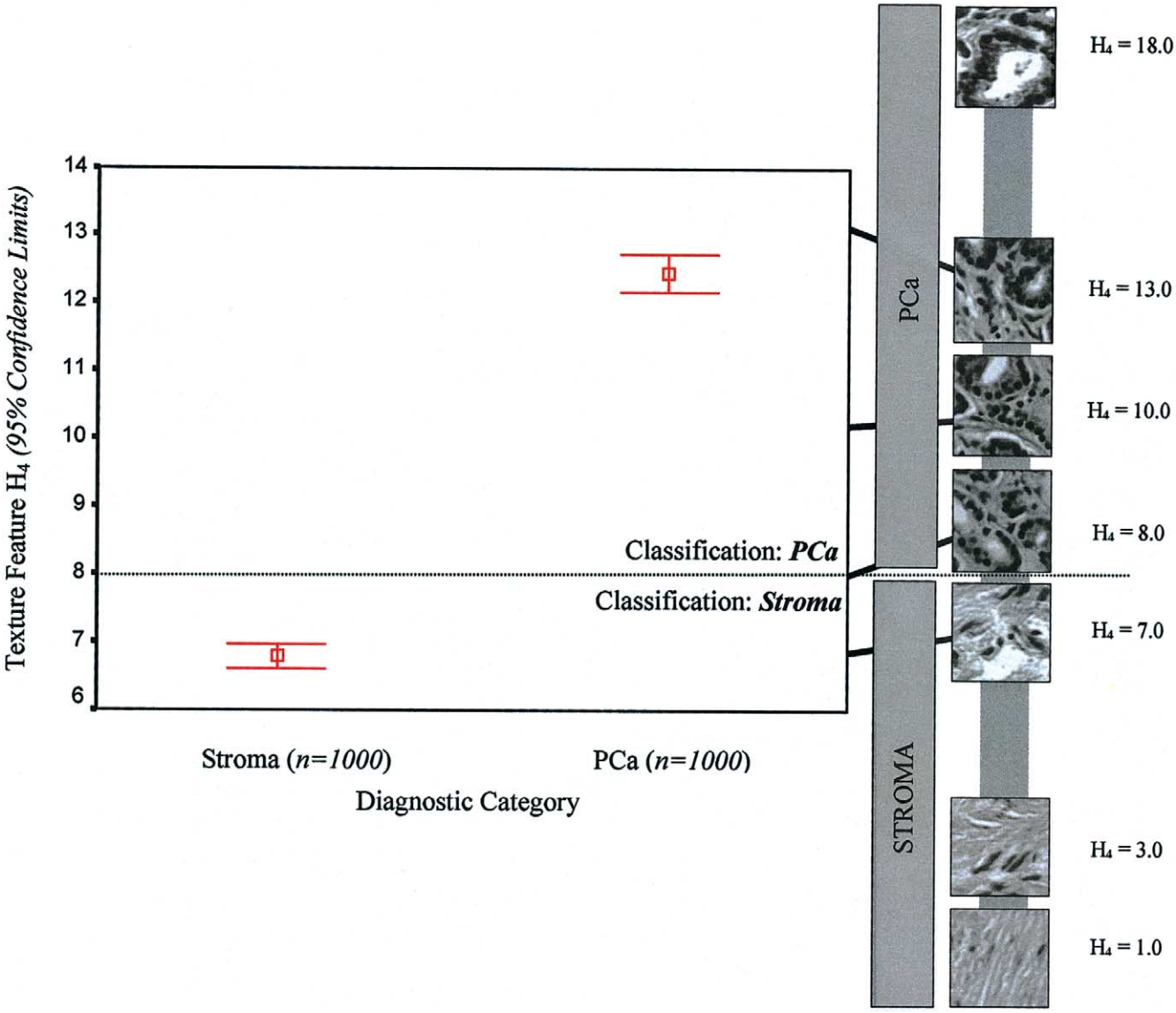

FIGURE 4. Threshold boundary for the discrimination of stroma and PCa.

mean epithelial region width of 50 pixels. The lumen objects identified were dilated by 50 pixels. Subsequent subtraction of the original lumen object defines the epithelial layer (Fig 2E). All subimages that contain some part of this object (and lumen) are classified as normal tissue and are highlighted in Figure 2F.

Classification of Stroma and PCa

Investigation of Haralick features suggested that Haralick 4 (H_4) was the most suitable for discriminating between stroma and PCa. Figure 4 shows the spectrum of change of H_4 observed for areas of stroma and PCa over the histological scenes (training set). A distinct change in image tissue composition between stroma ($H_4 < 8.0$) and PCa ($H_4 > 8.0$) can be seen. Figure 4 also highlights the variation in H_4 values for all example subimages in the training set ($n_{stroma} = 1000$ and $n_{PCa} = 1000$). A discrimination threshold was established at $H_4 = 8.0$ from examination of subimages from both stroma and PCa regions (training set). This threshold was set closer to the mean value of H_4 for stroma, to minimize the potential for misclassifying areas showing PCa as stroma and to reflect the visual change observed in Figure 4.

Analysis of Histological Scenes

In testing the system, tissue composition from 8 histological scenes (test set) was automatically identified based on the aforementioned criteria. Overall classification rates for the system in discriminating stroma, normal tissue, or PCa are given in Table 1. Selective detailed classifications are detailed in the following paragraphs and shown in Figures 5, 6, and 7.

TABLE 1. Classification Details for all Histological Scenes (Excluding Scan)

Scene	Dimension (pixels)	Tissue content	Subimages	Classification (%)
1*	2295×4407	Stroma, normal	968	82.5
2*	2277×5280	Stroma, normal, PCa	1144	88.9
3*	2345×4032	Stroma, PCa	920	72.6
4*	2408×4712	Stroma, normal, PCa	1128	79.9
5	2466×4815	Stroma, normal, PCa	1152	74.3
6	2420×4780	Stroma, normal, PCa	1128	88.4
7	3864×3717	Stroma, normal, PCa	1406	67.4
8	2368×4160	Stroma, normal	943	80.3
Scan	58877×42336	Stroma, normal, PCa	248,724	N/A

*Highlighted scenes are shown in Figures 5 and 6.
NOTE: Mean correct classification = 79.3% (excluding scan); total subimages classified = 8789 (excluding scan).

Scene 1 (Fig 5A and B)

The region of stroma (region A) was clearly identified by the system. The glandular regions (regions B and D) were well identified; small differences are visible, but the essence of region identification has been maintained. Some small regions were misclassified as PCa. It must be remembered that the process described here only suggests areas of abnormality. This false-positive result should be further investigated for confirmation or nonconfirmation at a higher power. The region of stroma (region C) was well defined, except for misclassification of the urethra area as normal prostatic acinar tissue. The correct classification rate for this scene was 82.5% (Table 2).

Scene 2 (Fig 5C and D)

The main region of PCa (region A) was clearly identified by the system, with the exception of 2 small regions of normal tissue. The region of stroma (region B) was clearly identified with its associated regions of PCa. The small region of normal tissue (region C) was generally defined but interpreted in a more fragmented nature by the system. The correct classification rate for this scene was 88.9% (Table 2).

Scene 3 (Fig 6A and B)

The main regions of PCa (region A) were clearly identified by the system; however, there is an overclassification of PCa. Stroma areas (region B) were well defined by the system. The correct classification rate for this scene was 72.6% (Table 2).

Scene 4 (Fig 6C and D)

The main region of PCa (region A) was clearly identified by the system; however, more stroma was identified than is evident on the pathologist's assessment. The main area of stroma (region B) was identified, together with its associated islands of PCa and normal tissue. The area of PCa (region C) was identified but is highly fragmented. Two small glandular areas (region D) exhibiting both PCa and normal tissue were identified. The correct classification rate for this scene was 79.9% (Table 2).

Scene 5 (Whole Slide Scanned Image)

Regions A and B represent the main areas of interest on this image. Both exhibited areas of PCa. Generally the PCa in region B was misclassified as normal tissue. The system misclassified regions C and D as Pca, essentially due to the existence of lymphocyte aggregates in these regions. The correct classification rate for this scene was not evaluated.

DISCUSSION

Accuracy and reproducibility in diagnosis is absolutely central. Automated imaging provides a potential platform for removing feature assessment subjectivity and identifying the appropriate diagnostic areas of the slide. In addition, automation possibly could provide a rapid method to screen histopathology for the study of morphological, histochemical, immunohistochemical, and hybridization biomarkers.

Previous work by our group highlighted the potential of image texture for mapping tissue abnormalities.[17] The present study has confirmed the role of texture algorithms in medium-power scanning of large-scale histological scenes for identifying normal/abnormal prostatic tissue components. It is clear from this work that tissue texture can accurately distinguish among stromal, normal, and PCa tissues and provides a means of locating important regions in medium-power scans, essential in the development of any automated system. The present study excludes histological grading or the identification of premalignant conditions, such as prostatic intraepithelial neoplasia (PIN).

The diagnosis of PCa is complex and based on many histological observations. The major criteria are infiltrative growth pattern, absence of a basal cell layer, and presence of macronucleoli. Texture analysis of medium-power scans has been shown to be capable of distinguishing between the first 2 criteria. Previous studies have demonstrated that the presence of nucleoli and other morphological features is an important indicator of malignancy (occurring in 94% of malignant cases).[22] Consequently, it is envisaged that an extension to the system mimicking that of a pathologist

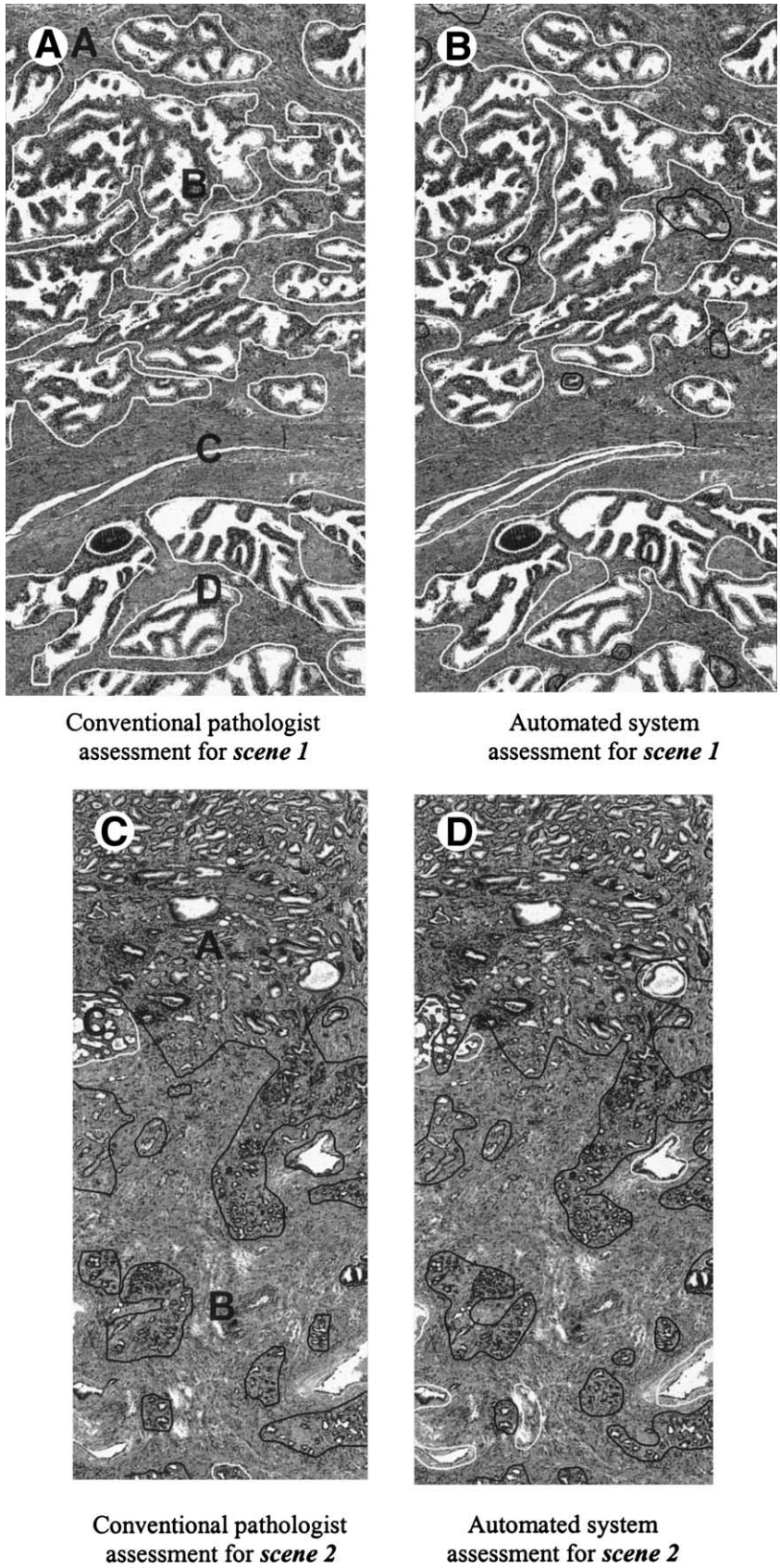

FIGURE 5. Histological assessment (scenes 1 and 2). White lines enclose normal tissue; black lines enclose PCa. (A) Conventional pathologist assessment for scene 1. (B) Automated system assessment for scene 1. (C) Conventional pathologist assessment for scene 2. (D) Automated system assessment for scene 2.

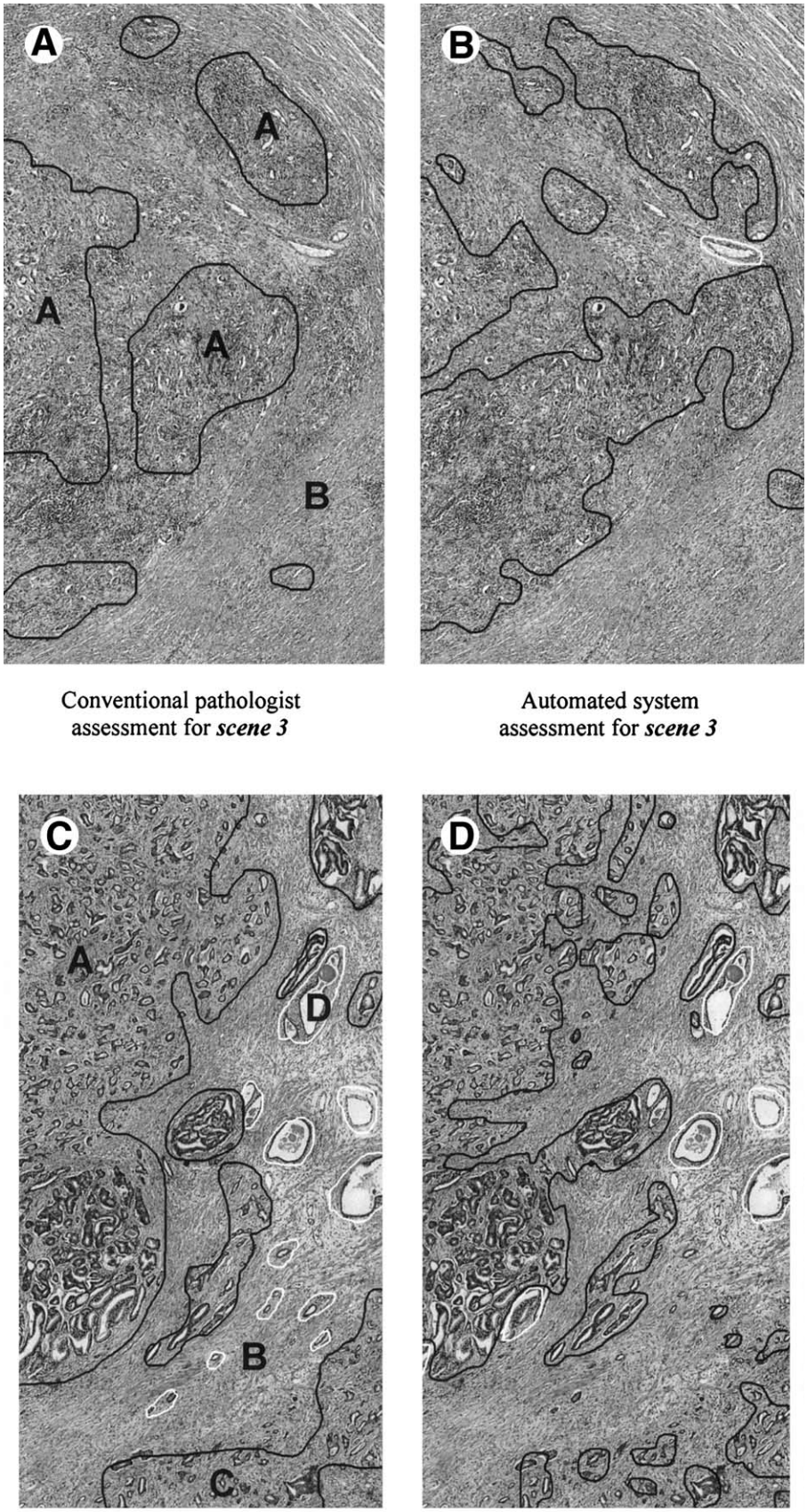

FIGURE 6. Histological assessment (scenes 3 and 4). White lines enclose normal tissue; black lines enclose PCa. (A) Conventional pathologist assessment for scene 3. (B) Automated system assessment for scene 3. (C) Conventional pathologist assessment for scene 4. (D) Automated system assessment for scene 4.

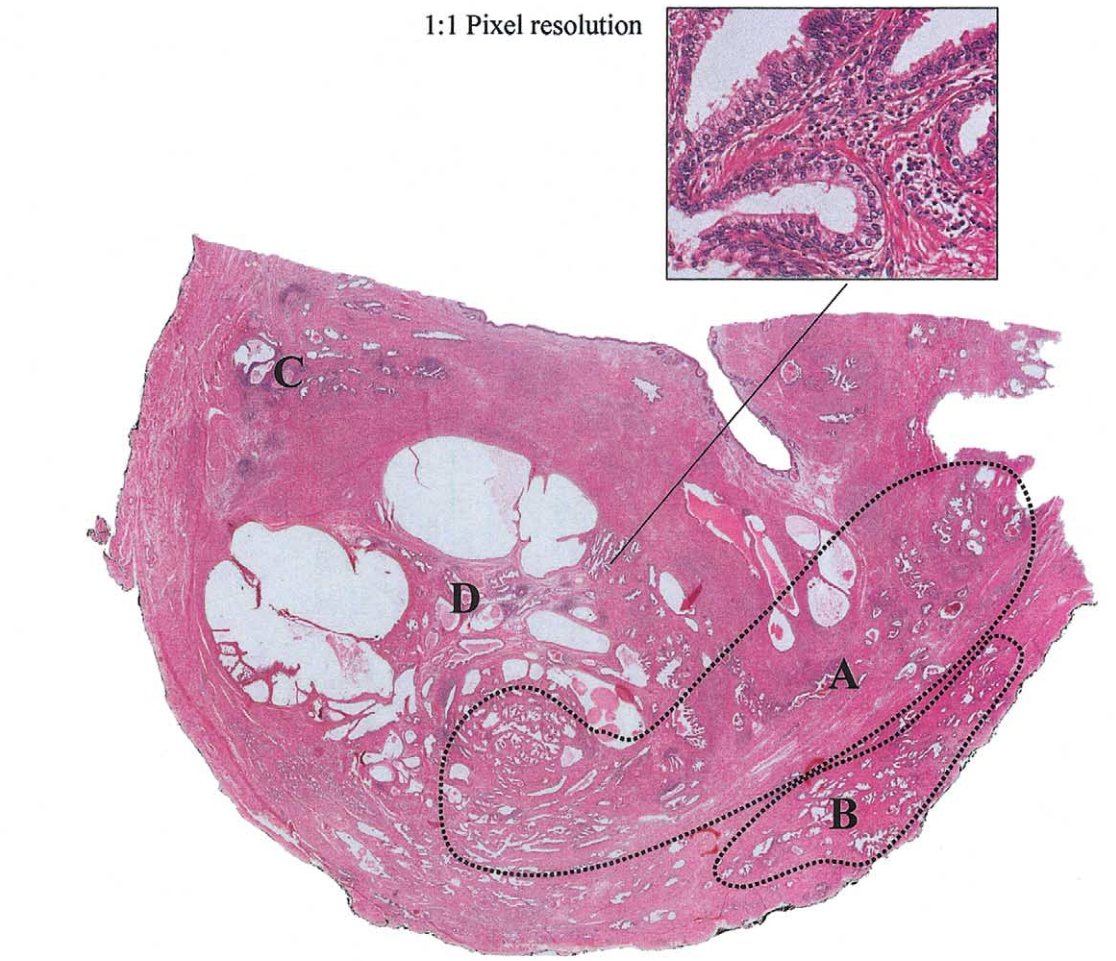

(a) Whole slide scan

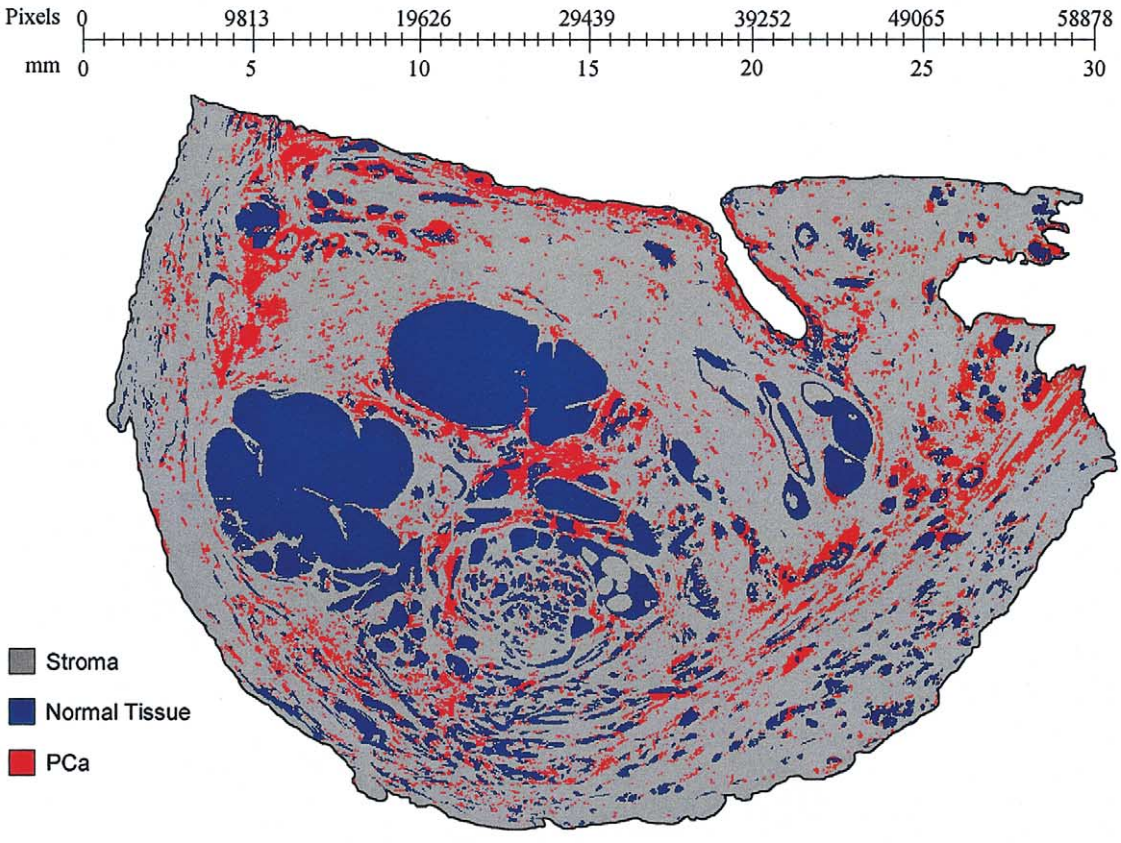

(b) Whole slide abnormality map

FIGURE 7. Whole slide processing. (A) Whole slide scan. (B) Whole slide abnormality map.

TABLE 2. Classification Matrix for Histological Scenes

			Predicted group membership		
	Actual group	Subimages	Stroma	Normal	PCa
Scene 1	Stroma	408	318 (77.9%)	80 (19.6%)	10 (2.4%)
	Normal	560	49 (8.9%)	481 (85.7%)	30 (5.4%)
	PCa	0	0 (0.0%)	0 (0.0%)	0 (0.0%)
			Total correct classification = 82.5%		
Scene 2	Stroma	516	433 (83.9%)	20 (3.9%)	63 (12.2%)
	Normal	24	0 (0.0%)	21 (87.5%)	3 (12.5%)
	PCa	604	28 (4.6%)	12 (19.7%)	564 (93.4%)
			Total correct classification = 88.9%		
Scene 3	Stroma	516	433 (83.9%)	20 (3.9%)	63 (12.2%)
	Normal	24	0 (0.0%)	21 (87.5%)	3 (12.5%)
	PCa	604	28 (4.6%)	12 (19.7%)	564 (93.4%)
			Total correct classification = 72.6%		
Scene 4	Stroma	627	479 (76.4%)	2 (0.3%)	146 (23.3%)
	Normal	0	0 (0.0%)	0.0 (0.0%)	0 (0.0%)
	PCa	293	104 (35.5%)	0 (0.0%)	189 (64.5%)
			Total correct classification = 79.9%		

would be beneficial, whereby confirmation of all areas of PCa would be examined at higher power.

Clearly, the classification of PIN should be considered in an extension to this investigation. The classification PIN is complicated by its segregation into low-grade/high-grade forms with its varying composition described as tufting, micropapillary, cribriform, or flat. Texture analysis will be unable to classify these compositions well, and a combined technique with glandular morphology will be needed. Texture analysis may also provide an approach for histological grading. This is suggested in Figure 4, which shows a spectrum of differentiation with respect to H_4.

Many established methods exist for the classification of textured images. Unfortunately, most techniques assume that the textures are uniformly presented and captured in the same orientation. This is an unrealistic assumption for pathological sections. For applications such as the current system, texture analysis needs to be invariant to orientation. Genuine orientation invariance is extremely difficult to obtain. In achieving pseudoinvariance, texture features within this system are averaged over the four principal directions (0, 45, 90, and 135 degrees), thus minimizing direction effects. In all texture-based applications, invariance in the staining of sections and in the illumination when acquiring imagery is also important. It is impossible to ensure total consistency in the staining of sections, and knowledge of whether the slides used were batch-processed is not available. However, given these limitations, functionality was built into the image preprocessing technique to minimize these effects. Consideration of the classification results has shown that the variations in classification rate are essentially due to image complexity.

Image analysis technology is a powerful resource that can be exploited to provide objective decision support for diagnostic pathology. Research and development of automated systems in pathology has been gaining momentum, not only for the rapid processing and staining of tissue samples, but also for the automated analysis of images extracted from tissue microarrays and histological scenes. A prerequisite for histological diagnosis is that a representative region of tissue must be assessed. Because histological structures frequently extend over areas greater than that of a single camera field, it is necessary to mosaic an array of images to produce a histological scene (Figs 5 and 6). Many authors have considered using automated slide digitization in this manner for assessing histological scenes.[23,24] However, this is a time-consuming process; digitization of a 10 × 10 mm region of tissue takes 70 minutes (× 20 objective magnification). It also is subject to misalignment of neighboring images. New technologies for slide scanning have recently become available, such as the ScanScope slide scanning system (Aperio Technologies, Vista, CA). The Aperio system has the capability to scan microscope slides at × 20/× 40, reducing scanning times to minutes for an average slide. In this study, ScanScope was used to scan an entire piece of tissue for analysis. Processing this image presents certain challenges, including the following:

1. Most processing packages to date (including KS400) do not offer JPEG 2000 functionality. The image can be converted to other uncompressed formats; however, the resulting image will be many gigabytes in size (Table 3).
2. Process time for the study was around 5.5 hours, which is clearly impractical for a routine automated system. If such images are to be analyzed in this manner then the move to hardware-based systems is required. Making use of modern FPGA (field-programmable gate array) technology, for example, would result in a substantial speed increase with the move to real time image processing.

Texture is the visual cue perceived from the repetition of image patterns. Color visual cue is the result of the observation of a specific illuminant on a given

TABLE 3. Scanning Details for Histological Slide

Description	Value
Tissue (X dimension)	27 mm
Tissue (Y dimension)	19 mm
Compression	JPEG2000
Color depth	24 bit
Compression quality	30
Compression ratio	16.38
Image width	58,877 pixels
Image height	42,336 pixels
Image size	7,477,850,016 bytes
File size	456,416,687 bytes
Scanning resolution	54000 pixels/inch
Scanning Speed	40 mm^2/minute

surface using 3 different types of sensors (red, green, and blue [RGB]). Because images are obtained in 24-bit format from the scanner, the possibility for extending texture analysis into the RGB domain is possible. Processing each color band separately or deriving textural information from the luminance plane along with chrominance features has been shown to increase the accuracy of the classification process. Consequently, color information may play a role in improving the discriminative power of machine vision systems.

In conclusion, the diagnosis of PCa is complex and is based on many histological observations. The major criteria are infiltrative growth pattern, absence of a basal cell layer, and presence of macronucleoli. Texture analysis of medium-power scans has been shown to be capable of distinguishing between the first 2 criteria. Previous studies have shown that the presence of nucleoli and other morphological features is an important indicator of malignancy.[22] Consequently, it is obvious that full automation will require the identification of high-power clues for diagnostic confirmation. However, low-power scans provide the means of identifying key areas of the tissue section that require scrutiny at higher power.

Advances in automated imaging in histopathology will continue, and tissue texture is likely to have an important role. Future work will require close collaboration between pathologists, software engineers, and computer scientists. This not only will enhance our ability to rapidly analyze patient material in an objective way, but also will possibly identify new reliable markers of diagnosis and prognosis.

REFERENCES

1. The Institute of Cancer Research: Prostate cancer set to become the most common men's cancer within three years [press release]. May 27, 2002

2. O'Leary TJ, Tellado M, Bruckner SB, et al: PAPNET-assisted rescreening of cervical smears: Cost and accuracy compared with 100% manual rescreening strategy. JAMA 279:235-237, 1998

3. Patten SF, Lee JS, Nelson AC: NeoPath AutoPap 300 automated Pap screener system. Acta Cytol 40:45-52, 1996

4. Thompson D, Bartels PH, Bartels H, et al: Knowledge-based segmentation of colorectal histologic imagery. Anal Quant Cytol Histol 15:236-246, 1993

5. Hamilton PW, Thompson D, Sloan J, et al: Knowledge-guided segmentation and morphometric analysis of colorectal dysplasia. Anal Quant Cytol Histol 17:172-182, 1995

6. Bartels PH, Thompson D, Bartels H, et al: Machine vision–based histometry of premalignant and malignant prostatic lesions. Pathol Res Pract 191:935-944, 1995

7. Thompson D, Bartels PH, Bartels H, et al: Image segmentation of cribriform gland tissue. Anal Quant Cytol Histol 17:314-322, 1995

8. Anderson NH, Hamilton PW, Bartels PH, et al: Computerized scene segmentation for the discrimination of architectural features in proliferative lesions of the breast. J Pathol 181:374-380, 1997

9. Keenan S, Diamond J, McCluggage WG, et al: An automated machine vision system for the histological grading of cervical intraepithelial neoplasia (CIN). J Pathol 192:351-362, 2000

10. Baak JPA: The framework of pathology: Good laboratory practice by quantitative and molecular methods. J Pathol 198:277-283, 2002

11. Julesz B: Texture and visual perception. Sci Am 212:38-48, 1965

12. Richard WD, Keen CG: Automated texture-based segmentation of ultrasound images of the prostate. Comput Med Imaging Graph 20:131-140, 1996

13. Basset O, Sun Z, Mestas JL, et al: Texture analysis of ultrasonic images of the prostate by means of co-occurrence matrices. Ultrason Imaging 15:218-237, 1993

14. Christen R, Xiao J, Ninimo C, et al: Chromatin texture features in hematoxylin and eosin–stained prostate tissue. Anal Quant Cytol Histol 15:383-388, 1993

15. Bartels PH, Montironi R, Hamilton PW, et al: Nuclear chromatin texture in prostatic lesions: 1. PIN and adenocarcinoma. Anal Quant Cytol Histol 20:389-396, 1998

16. Bartels PH, Montironi R, Hamilton PW, et al: Nuclear chromatin texture in prostatic lesions: 2. PIN and malignancy-associated changes. Anal Quant Cytol Histol 20:397-406, 1998

17. Hamilton PW, Bartels PH, Thompson D, et al: Automated location of dysplastic fields in colorectal histology using image texture analysis. J Pathol 182:68-75, 1997

18. Hamilton PW, Bartels PH, Montironi R, et al: Automated histometry in quantitative prostate pathology. Anal Quant Cytol Histol 20:443-460, 1998

19. Bartels PH, Bartels H, Montironi R, et al: Machine vision in the detection of prostate lesions in histologic sections. Anal Quant Cytol Histol 20:358-364, 1998

20. Haralick RM, Shanmugsm K, Dinstein I: Texture features for image classification. IEEE Trans Syst Man Cybern 3:610-621, 1973

21. Bartels PH, Bartels H, Montroni R, et al: Machine vision in the detection of prostate lesions in histologic sections. Anal Quant Cytol Histol 20:358-364, 1998

22. Varma M, Lee MW, Tamboli P, et al: Morphologic criteria for the diagnosis of prostatic adenocarcinoma in needle biopsy specimens. Arch Pathol Lab Med 126:554-561, 2002

23. Thompson D, Richards D, Bartels H, et al: Multimegapixel images in histopathology. Anal Quant Cytol Histol 23:169-177, 2001

24. Leong FJW-M, McGee JO'D: Automated complete slide digitization: A medium for simultaneous viewing by multiple pathologists. J Pathol 195:508-514, 2002